THE JOURNAL OF BIOLOGICAL CHEMISTRY
Vol. 269, No. 5, Issue of February 4, pp. 3703–3710, 1994
Printed in U.S.A.

De Novo Autophagic Vacuole Formation in Hepatocytes Permeabilized by *Staphylococcus aureus* α-Toxin

INHIBITION BY NONHYDROLYZABLE GTP ANALOGS*

(Received for publication, June 16, 1993, and in revised form, September 7, 1993)

Motoni Kadowaki‡, Rina Venerando§, Giovanni Miotto§, and Glenn E. Mortimore‡

From the ‡Department of Cellular and Molecular Physiology, College of Medicine, The Pennsylvania State University, Hershey, Pennsylvania 17033 and the §Dipartimento di Chimica Biologica, Università Degli Studi di Padova, Padova 35121, Italy

The role of GTP-binding proteins in autophagic vacuole formation was investigated in isolated rat hepatocytes permeabilized by α-toxin from *Staphylococcus aureus*, an agent which creates stable plasma membrane channels allowing exchange of small (≤1000 Da) molecules. Vacuole formation was monitored from the uptake of ^{125}I-tyramine-cellobiitol (^{125}ITC) into osmotically sensitive vacuoles isolated on colloidal silica density gradients. Separation was based on an established observation that autophagic vacuoles are retained in a heavy midgradient band when samples are layered, but are selectively shifted to dense fractions when they are previously dispersed in the gradient material. The vacuolar uptake of ^{125}ITC was concentration-dependent and required exogenous ATP: 94% was directly mediated by sequestration; 6% was acquired by fluid-phase endocytosis as monitored by [*carboxyl*-^{14}C]dextran-carboxyl. Although the amino acid control of proteolysis was lost, addition of the nonhydrolyzable GTP analog GTPγS (as well as GMP-PNP) decreased fractional rates of direct vacuolar ^{125}ITC uptake and long-lived proteolysis by similar amounts (1.02–1.03% h^{-1}), substantiating the notion that the effects were the direct result of autophagic inhibition. These and associated findings, supported by quantitative electron microscopy, indicate the presence of ongoing macro- and microautophagy in α-toxin-permeabilized cells and suggest that one or more GTP-binding proteins is required in macroautophagic vacuole formation.

Autophagy is a highly conserved, physiologically regulated intracellular process that plays a major role in the turnover of long-lived proteins, RNA, and other macromolecular constituents of cytoplasm (reviewed in Refs. 1 and 2). The overt or macroautophagic vacuole is under direct control by amino acids (3, 4) and derives its membranes from the rough endoplasmic reticulum (4). Owing in part to its complexity and inaccessibility to external probes, little is known of the molecular steps in vacuole formation. Microinjection (5) and electropermeabilization (6) have been used to introduce labels into cells that can be followed into newly formed vacuoles. But since the pores are transient, observations are limited to events that occur after membrane resealing. Thus, the question of whether autophagic vacuoles can form in permeabilized cells before the pores reseal remains unanswered.

GTP-binding proteins have been implicated in an increasing number of membrane events such as endosome fusion, vesicle formation by the endoplasmic reticulum, the Golgi/secretory pathway, exocytosis, and glucose transporter translocation (7–13); it is also possible that GTP-binding proteins play a role in autophagic vacuole formation. The question would be testable if the process could be demonstrated in suitably permeabilized cells. In this study with isolated rat hepatocytes, α-toxin from *Staphylococcus aureus* was chosen as the permeabilizing agent because it forms circular hexamers in the plasma membrane with ≈2 nm channels that limit exchange to molecules of approximately 1000 Da or smaller (14). Such pores would admit nucleotides and residualizing probes without loss of cell proteins, a desirable, possibly necessary, condition for evaluating autophagically mediated proteolysis.

EXPERIMENTAL PROCEDURES

Materials—Highly purified α-toxin from *S. aureus* (23.8 rabbit hemolytic units per μg), prepared according to Harshman *et al.* (15), was a generous gift of Dr. Sidney Harshman, Vanderbilt University School of Medicine. ATP (disodium salt), creatine phosphate, creatine phosphokinase, GTP, GTPγS,[1] GDPβS, and GMP-PNP were obtained from Sigma; 3-methyladenine from Aldrich; and collagenase (*Clostridium histolyticum*) from Boehringer Mannheim. Ludox HS-40 was a gift of E. I. du Pont de Nemours; povidone (polyvinylpyrollidone) was purchased from Thomas; Na^{125}I (17 Ci/mg), [γ-^{32}P]ATP (10 Ci/mmol), and [*carboxyl*-^{14}C]dextran-carboxyl (M_r = 50,000–70,000) from DuPont NEN; and bovine plasma albumin (fraction V) from Pentex, ICN. ^{125}I-Tyramine-cellobiitol was synthesized according to Pittman and Taylor (16), and ^{32}P-labeled glucose 6-phosphate was made as described by Arion *et al.* (17).

Hepatocyte Preparation and Permeabilization—Male rats of the Lewis strain (Harlan Sprague-Dawley, Indianapolis), weighing 200–300 g, served as hepatocyte donors. They were maintained in a temperature/light-controlled room with free access to water and fed a standard 35% casein diet in a synchronous feeding regimen as detailed elsewhere (18). Parenchymal cells were isolated 18 h after the start of the last feeding by the collagenase method of Seglen (19), modified slightly by Venerando *et al.* (20). In experiments with intact hepatocytes, cells were suspended at a density of 2 × 10^6/ml in Krebs-Ringer bicarbonate buffer containing 6 mM glucose and 0.5% albumin; oxygenation and pH (7.4 at 37 °C) were maintained by gassing with O_2:CO_2 (95:5, v/v). Cell viability was monitored by trypan blue exclusion.

In the preparation of permeabilized hepatocytes, cells were first isolated as above and immediately resuspended at the above cell density in the following cytosolic buffer (mM): NaCl, 20.0; KCl, 100.0; $MgSO_4$, 5.0; NaH_2PO_4, 0.96; $NaHCO_3$, 20.0; $CaCl_2$, 0.49; EGTA, 1.0; and 2% albumin (pH 7.2 at 37 °C under the same gas mixture). Free Ca^{2+} was main-

* This work was supported by United States Public Health Service Grant DK 21624 (to G. E. M.) with additional funding from Sigma Tau (to R. V. and G. M.). The costs of publication of this article were defrayed in part by the payment of page charges. This article must therefore be hereby marked "*advertisement*" in accordance with 18 U.S.C. Section 1734 solely to indicate this fact.

[1] The abbreviations used are: GTPγS, guanosine 5′-*O*-(3-thiotriphosphate); GDPβS, guanyl-5′-yl thiophosphate; GMP-PNP, guanyl-5′-yl imidodiphosphate; ^{125}ITC, ^{125}I-tyramine-cellobiitol; M + L, mitochondrial-lysosomal fraction; β-hexosaminidase, *N*-acetyl-β-D-glucosaminidase; AVi, initial/nascent macroautophagic vacuole (autophagosome); AVd, degradative/digestive macroautophagic vacuole (autolysosome); ER, endoplasmic reticulum.

tained at 0.18 μM by the addition of 1 mM EGTA (21). α-Toxin (in 100 mM NaH_2PO_4, pH 7.2, at indicated dosages) was then added; after standing for 5 min at 37 °C, the cells were washed once and resuspended in fresh cytosolic buffer. Cells were incubated at a density of 2 × 10^6 cells/ml except in the ^{125}ITC and radiolabeled dextran-carboxyl uptake experiments where 10^7 cells/ml were used. ATP was added by means of a regenerating system consisting of 1.5 mM ATP, 5 mM creatine phosphate, and 5 units/ml creatine phosphokinase (21).

^{125}ITC and [carboxyl-^{14}C]Dextran-Carboxyl Uptake—Permeabilized cells (10^7/ml) were incubated for 60 min (90 min in Fig. 6) in 3 ml of cytosolic buffer at 37 °C. Five μCi of ^{125}ITC or 13 μCi of [*carboxyl*-^{14}C]dextran-carboxyl were added at 30 min, and 1.0-ml samples were taken at 60 min, washed twice with 5 ml of ice-cold 0.25 M sucrose-1 mM EDTA (pH 7.4), and then homogenized in 2 ml of the same solution with 40 strokes of a tightly fitting, Dounce tissue grinder (Kontes). The M + L fraction was separated by differential centrifugation (22) and then resuspended in the sucrose-EDTA solution for particle separation on colloidal silica density gradients. Recovery of the lysosomal marker β-hexosaminidase in the M + L averaged 0.70 of the total; the balance was in the M + L (0.2) and nuclear (0.1) fractions.

The gradient medium consisted of 7.0% Ludox (colloidal silica) and 4% povidone in 0.25 M sucrose (density gradient grade, Schwarz/Mann) at pH 7.2, prepared as described earlier (22). Samples of the M + L fractions (3.83 mg of protein in 0.135 ml) were either layered on the chilled gradient medium (4.6 ml) or thoroughly dispersed within it before centrifugation. The latter was carried out at 16,900 rpm for 60 min in a Sorvall RC-5B centrifuge with an SV-80 vertical rotor. In experiments where unlabeled M + L from intact liver was mixed with labeled M + L from incubated cells, a vertical rotor of larger capacity (SS-90) was employed. In these instances, 1.0-ml samples containing 28.4 mg of protein were used, and centrifugation was carried out at 18,000 rpm for 150 min. In both conditions, fractions were collected by vertical displacement and counted as described below.

In computing differences in intravacuolar label between layered and dispersed gradients in the lower fractions (typically 1–11) of Figs. 4 and 5 and Table II, correction was made for the presence of extra label in water surrounding the particles. Control gradients showed that, with dispersion, free label is evenly distributed along the gradient whereas with layering it remains largely in the upper fractions, decreasing gradually to zero by fractions 10 and 11. Since the bottom fractions (1 and 2) in layered gradients were devoid of radioactivity, the total quantity of extraneous free label in fractions 1–11 was determined by the difference in radioactivity in the initial fractions multiplied by the 11 fractions of the dispersion shift.

Analytical Procedures—β-Hexosaminidase, citrate synthase, galactosyltransferase, and protein in the gradient fractions were determined according to Surmacz *et al.* (22). For the analysis of free valine, medium and cell samples were deproteinized in 6% perchloric acid; the amino acids then were dansylated and assayed by high performance liquid chromatography as described by Venerando *et al.* (20). Cell and medium samples with ^{14}C were dissolved in 1 N NaOH, neutralized, and counted with Liquiscint (National Diagnostics, Inc.) in a Beckman LS 7800 liquid spectrometer; results were expressed as disintegrations per min. Gradient samples were handled similarly except that they were initially dissolved in Triton X-100 and ethanol. All ^{125}I samples were counted directly in a Beckman Gamma 5500B system.

All data from more than two experiments were expresssed as means ± S.E. The significance of differences between means was evaluated by the Student's *t* test; values of *p* greater than 0.05 were considered not significant.

RESULTS AND DISCUSSION

Characteristics of α-Toxin-permeabilized Cells—As determined from the intracellular hydrolysis of externally added glucose 6-phosphate, α-toxin effectively permeabilized the hepatocyte over an 8-fold range of dosage (Fig. 1), a finding in agreement with McEwen and Arion (23). Because α-toxin-induced pores are sufficiently large to allow exchange of nucleotides across the plasma membrane (13), the possibility was considered that proteolysis would be adversely affected by a diminished energy supply. For this reason, the net release of valine, largely reflecting proteolysis, was evaluated in the presence and absence of an ATP regenerating system. Time courses are shown in Fig. 2 for the two highest doses, 65 and 130 units/ml. After a rapid initial release (attributed to the breakdown of protein previously sequestered in autophagic vacuoles), rates from 30 to 90 (or 120 min, not shown) were constant in the presence of external ATP but appreciably decreased in its absence. With doses of α-toxin of 65 units/ml and lower, 1.5 mM ATP yielded optimal results since rates of valine release between 30 and 90 min were virtually identical in two series of α-toxin experiments (65 units/ml) with external ATP levels of

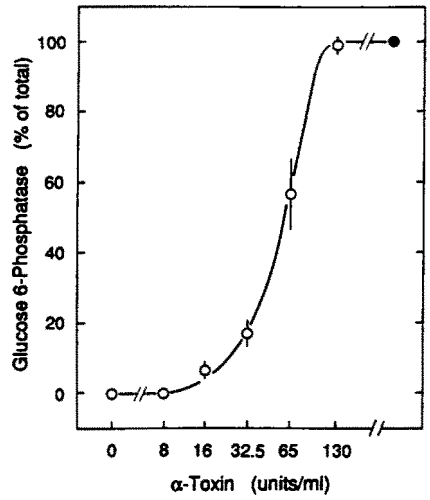

FIG. 1. **Permeabilization of isolated hepatocytes exposed to graded levels of α-toxin, determined from the accessibility of glucose-6-phosphatase activity to external glucose 6-phosphate.** Cells were treated with α-toxin (see "Experimental Procedures") and immediately incubated with 2 mM [^{32}P]glucose 6-phosphate for 5 min at 37 °C. The $^{32}P_i$ produced was assayed as [^{32}P]phosphomolybdate according to McEwen and Arion (23). ●, total activity after solubilizing cells with 0.2% deoxycholate. Data are means ± S.E. of three experiments.

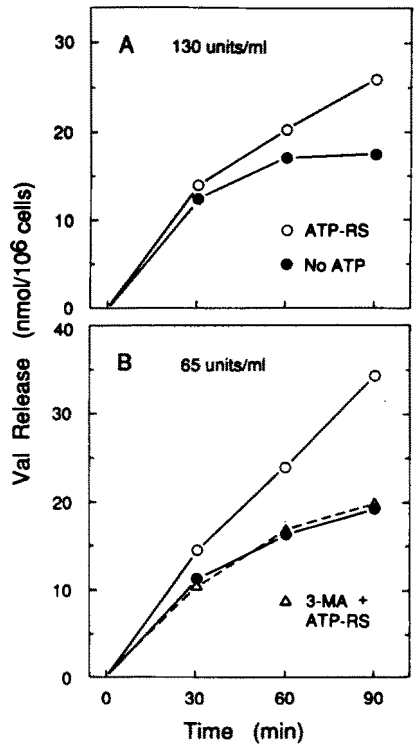

FIG. 2. **Effects of α-toxin dosage, ATP, and 3-methyladenine (*3-MA*) on the net release of valine from permeabilized liver cells.** Isolated cells were exposed to α-toxin at 130 (*A*) and 65 (*B*) units/ml as described under "Experimental Procedures." Total valine release, predominantly a reflection of proteolysis, was analyzed in cells (and medium) incubated with and without an ATP regenerating system (*ATP-RS*); the concentration of 3-methyladenine was 10 mM.

0.75, 1.5, 3, and 6 mM (not shown).

3-Methyladenine, a potent inhibitor of AVi formation (24), was employed preliminarily as a test for induced autophagy. As shown in Fig. 2 (*lower panel*), the agent strongly inhibited valine release in the presence of ATP, suggesting that new autophagic vacuoles were formed between 30 and 90 min.

Electron microscopy revealed no evidence of cytotoxicity at 32.5 and 65 units/ml of α-toxin as judged by the presence of normal microvilli and absence of plasma membrane blebbing. We did, though, observe fragmentation and dilation of rough and smooth ER. This was associated with a shift of ER to the cell periphery and clustering of mitochondria centrally (Fig. 3). These changes appeared gradually but were distinctly noticeable by 20 min, visible by light microscopy as a "halo" beneath the plasma membrane. Macroautophagic vacuoles were observed in cells permeabilized with 32.5 (Fig. 3) and 65 units/ml α-toxin (not shown). Although the number of vacuoles was considerably smaller than that induced by amino acid deprivation in the intact liver (3, 4), their principal features remained the same. Because the rough ER is the source of forming membranes for AVi (4), its disorganization with increasing levels of toxin might have contributed to the decrease of proteolysis noted in Fig. 2 (see also Table I and Fig. 4).

We have no clear idea of the nature of the disruptive effect of α-toxin on the ER. Two possibilities, though, may be considered. First, while the α-toxin hexamer channel is too small to admit a monomer directly (14), membrane-bound toxin would probably be internalized by endocytosis. But whether this uptake would affect the ER is not known. Second, the changes might have arisen indirectly from ionic alterations or the loss of other small molecules as a consequence of the permeabilization. We excluded the notion that the high Cl^- in the cytosolic buffer was responsible by switching to glutamate buffer (25); no effect on valine release was found. In other experiments, no improvement was seen with the addition of 5 mM GSH.

Finally, it should be mentioned that because the ER fragmentation was distributed evenly among cells at 32.5 and 65 units/ml, it is probable that channel formation was random. Thus, the dose-response curve of α-toxin permeabilization in Fig. 1 may be interpreted as corresponding to the number of channels per cell rather than to varying mixtures of intact and maximally permeabilized cells.

Effect of α-Toxin on Amino Acid Control of Proteolysis—Since regulatory amino acids as a group are capable of inhibiting hepatic macroautophagy and proteolysis almost completely at 4 times normal plasma levels (3, 18), we tested their effectiveness in permeabilized cells. In Table I, intact cells elicited responses that agreed closely with effects in perfused livers of similar rats (18), assuming 10^8 cells per g of liver in the fed rat (19). While inhibition was found at a dose of 16 units/ml, it was abruptly lost at 32.5 and 65 units/ml despite electron microscopic evidence of ongoing macroautophagy (Fig. 3). The reason for this is not immediately apparent. Results of recent studies have suggested that amino acids mediate their inhibitory effects from plasma membrane recognition sites (26, 27). If so, it is possible that the inhibitory signal is conveyed through a second messenger, acting at autophagic loci throughout the cell. If this notion proves correct, a conceivable explanation is that a putative signal had leaked from the cell; other explanations, of course, are possible.

The suggestion from results in Table I that α-toxin exerted a stronger suppression on amino acid regulation than on rates of proteolysis in the absence of added amino acids raised the possibility that different mechanisms were involved. It is of interest that a plot of V/S *versus* V in Fig. 4*A* (where V is the inhibition of proteolysis in Table I and S the dose of toxin minus a threshold dose of 13.5 units/ml) yields an apparent K_m that is nearly twice that from a similar plot of the effect of the toxin on amino acid inhibition (Fig. 4*B*); both are highly linear. The threshold value or lag in response to dosage has been documented (28) and suggests that a critical level of toxin binding is needed before hexamers (with channels) are formed. Although

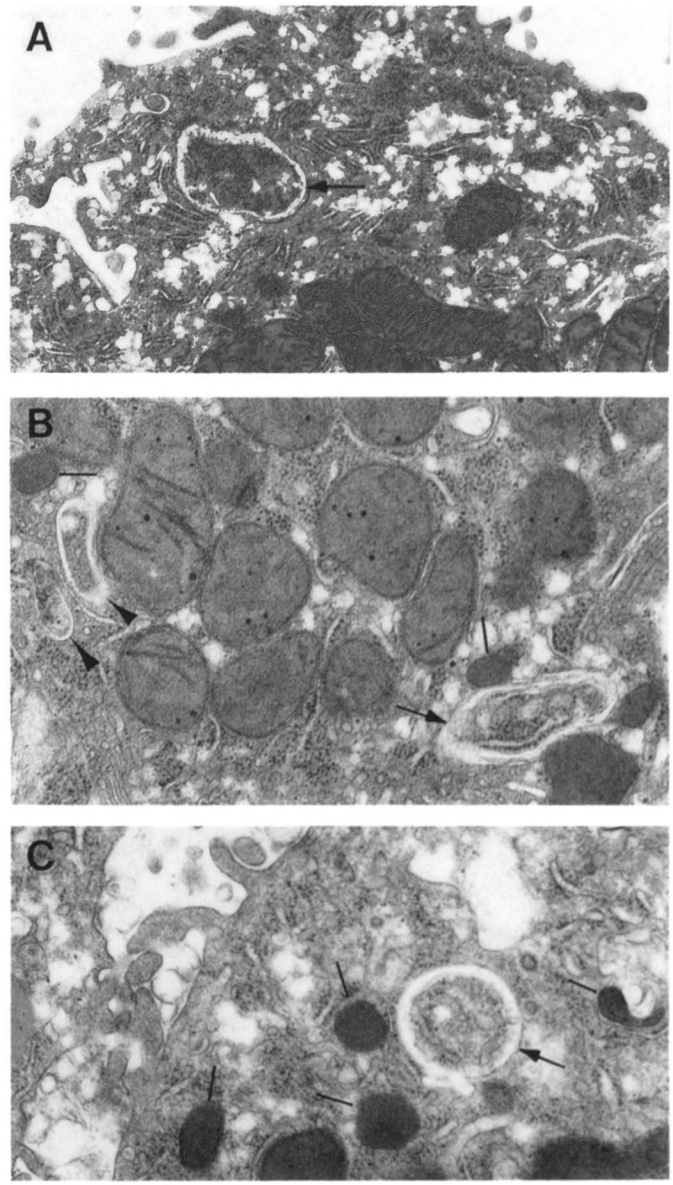

FIG. 3. **Electron micrographs of permeabilized hepatocytes.** Isolated hepatocytes were exposed to 32.5 units/ml α-toxin and incubated for 20 (*A* and *B*) and 60 min (*C*) with an ATP regenerating system. The cells were prepared for electron microscopy as described earlier (3, 40), and thin sections were examined with a Philips 400 electron microscope. *A*, a typical response to α-toxin showing fragmented rough ER at the cell periphery. An AVi containing numerous ribosomes and a few membranes is seen (*arrow*). It closely resembles AVi in the intact hepatocyte except for its angularity; this, and the elongated shapes in *A* and *B*, could be a consequence of the ER fragmentation. Note the normal appearing mitochondria. ×15,625. *B*, an elongated AVi with sequestered rough ER (*arrow*) and two probable AVi (*arrowheads*). Note secondary lysosomes (*lines*) and dilated/fragmented smooth ER at the bottom of the figure. ×30,800. *C*, an AVi containing ribosomes and smooth membranes (*arrow*) together with several secondary lysosomes (lines) in a cell incubated for 60 min. ×25,500. AVd were also present, but not shown, as were many profiles that could represent microautophagic vacuoles (type A secondary lysosomes) previously described in the intact cell (40). Many of these, however, were too unusual in shape to identify with certainty. Since nascent microautophagic vacuoles are believed to arise from the smooth ER (40), it is possible that the effect of α-toxin on the ER (see text) contributed to these alterations.

TABLE I

Effect of α-toxin on the proteolytic responsiveness of the isolated rat hepatocyte to regulatory amino acids

Isolated hepatocytes were permeabilized with graded doses of α-toxin and incubated at a density of 2×10^6 cells/ml. Proteolysis was measured from the release of valine with and without regulatory amino acids; after 30 min of incubation, 20 μM cycloheximide was added, and samples were taken at 37 and 47 min for valine analysis as described under "Experimental Procedures." Although widely used in other applications, isotopic procedures were not feasible here because the need to maintain low cell densities during the incubations (20) would have limited the amount of label released to levels difficult to measure. The Reg AA mixture comprised Leu, Gln, Tyr, Pro, Met, His, and Trp at 4 times (×) normal plasma concentrations (18). Values are means ± S.E. of 3–11 experiments.

α-Toxin	Proteolysis		
	No amino acids (A)	4× regulatory amino acids (B)	A − B
units/ml	*nmol Val min⁻¹/10⁶ cells*		
0	0.879 ± 0.042	0.423 ± 0.032	0.456[a]
16	0.699 ± 0.065	0.410 ± 0.056	0.289[b]
32.5	0.386 ± 0.029	0.332 ± 0.035	0.054
65	0.286 ± 0.030	0.276 ± 0.020	0.010
130	0.238 ± 0.012		

[a] $p < 0.001$.
[b] $p < 0.02$.

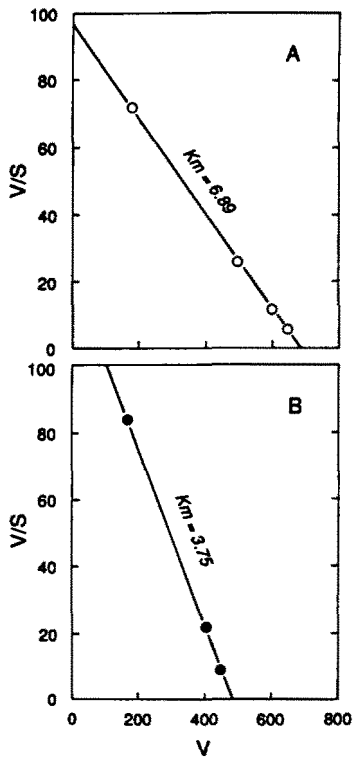

FIG. 4. **Suppressive effects of graded doses of α-toxin on proteolysis in isolated hepatocytes incubated in the presence and absence of regulatory amino acids.** *A*, a plot of *V/S versus V* of the inhibition of proteolysis by graded doses of α-toxin in the absence of added amino acids using data from Table I. *V* denotes the suppressive effect on proteolysis; *S* is the dose of α-toxin *minus* a threshold value of 13.5 units. The apparent K_m is 6.89 units (+ 13.5 units); V_{max} is 675 nmol of Val $min^{-1}/10^6$ cells; $r = 1.000$. *B*, a plot of *V/S versus V* of decreasing amino acid effectiveness with increasing α-toxin. *V* represents decreases in the inhibitory effect of regulatory amino acids at 4 times normal plasma concentrations with α-toxin (computed from data in Table I); *S* is the dose of toxin *minus* a threshold value of 14 units. The apparent K_m is 3.75 units (+ 14 units); V_{max} is 481 nmol of Val $min^{-1}/10^6$ cells; $r = 1.000$.

TABLE II

Effects of GTPγS and 3-methyladenine (3-MA) on the volume density of autophagosomes (AVi) in isolated rat hepatocytes permeabilized by α-toxin

Isolated hepatocytes were permeabilized with 32.5 units/ml α-toxin and incubated for 45 min with an ATP regenerating system under the conditions below. Following the incubation, the cells were fixed and embedded by the same procedures used in Fig. 3. Thin sections were then cut, stained (3), and examined with a Philips 300 or 400 electron microscope. The stereological methods used were the same as those described earlier (3, 40) except for the method of sampling. To evaluate sampling error in control cells, three areas were randomly selected from the blocks and, from each, 12 micrographs (×16,140) were systematically produced as in earlier studies (3, 40). Fractional AVi volumes were then determined by the point method through a grid of interesecting lines (3, 40). Since virtually no AVi were present after treatment, the 24 micrographs from each of the test conditions were treated as single groups. Absolute AVi volumes were computed from the volume of cytoplasm which was taken to be 647 μl/10^8 cells (legend to Table V). Rates of long-lived proteolysis, determined between 30 and 90 min with and without 1 mM GTPγS as in Table IV, were, respectively, 0.978 and 2.052 μmol of Val $h^{-1}/10^8$ cells. These values are representative of corresponding rates in Tables IV and V.

Condition	Volume density of AVi		
	% cytoplasm	*μl/10⁸ cells*	*% inhibition*
No additions	0.249[a]	1.611	0
1 mM GTPγS	0.015	0.097	94.0
10 mM 3-MA	0.008	0.052	96.8

[a] Mean of three randomly selected areas (see legend), which are: 0.2427, 0.2377, and 0.2667.

these plots provide no explanation for the underlying mechanisms, the difference in apparent K_m values is consistent with the existence of at least two effects of the toxin and clearly confirms the impression that amino acid regulation is the more sensitive of the two. But whether the loss of regulation is the direct result of permeabilization is not known.

Inhibition of AVi Formation by GTPγS and 3-Methyladenine in α-Toxin-permeabilized Hepatocytes—The effectiveness of GTPγS in suppressing macroautophagy was evaluated by quantitative electron microscopy, and the results were compared with those of 3-methyladenine, an established inhibitor of AVi formation (24). AVi rather than AVd vacuoles were employed as endpoints because AVi are readily identified and, hence, more accurately measured, especially at low volume densities. Small AVd and large dense bodies, for example, are frequently difficult to distinguish (3). The results in Table II show that both GTPγS and 3-methyladenine are highly effective inhibitors, suppressing the volume density of AVi in control cells by 94–97%; no AVd were seen after treatment. The relevance of the GTPγS effect will be discussed below in relation to the findings in Table V.

Distribution of ^{125}ITC and Subcellular Particles from Permeabilized Hepatocytes in Colloidal Silica Gradients—The formation of new autophagic vacuoles in isolated hepatocytes permeabilized with 32.5 units/ml of α-toxin was monitored with the use of ^{125}ITC, a stable probe that is retained within membrane-bound spaces (29). Vacuoles were identified on the basis of previously characterized features of colloidal silica density gradients (22, 30, 31). When the samples are layered on the gradient medium, autophagic vacuoles in M + L samples from rat liver have been shown to be retained by a heavy midgradient band consisting largely of mitochondrial and microsomal particles (fractions 14–18 in Fig. 5); when dispersed, the vacuoles are selectively shifted downward to dense fractions. By contrast, Golgi vesicles and some endosomes either fail to move or shift upward to lower densities while small lysosomes remain in the dense region of the gradient. Thus, differences between sample layering and dispersion in the amount of lysosomal marker in the dense region will directly reflect autophagy.

The retention is believed to result from a "sieving" effect of

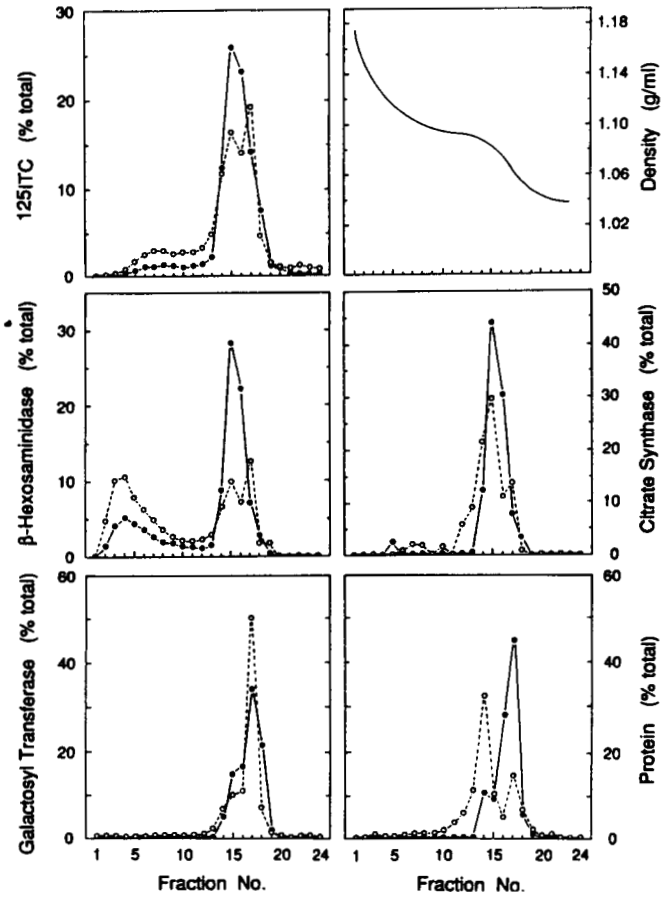

FIG. 5. **Distributions of ^{125}ITC, density, and protein together with enzyme markers for lysosomes (β-hexosaminidase), mitochondria (citrate synthase), and Golgi particles (galactosyltransferase) in hybrid M + L fractions separated in colloidal silica gradients.** Isolated hepatocytes were permeabilized with 32.5 units/ml α-toxin and incubated for 60 min with an ATP regenerating system; ^{125}ITC was added at 30 min. M + L fractions from the incubated cells were mixed with similar fractions from unlabeled intact liver at a ratio of 1:8 (v/v), respectively. Samples (1.0 ml) of the pooled M + L fractions were then applied to the gradient material by layering (●) or dispersion (○). Centrifugation was carried out in a Sorvall SS-90 rotor as described under "Experimental Procedures."

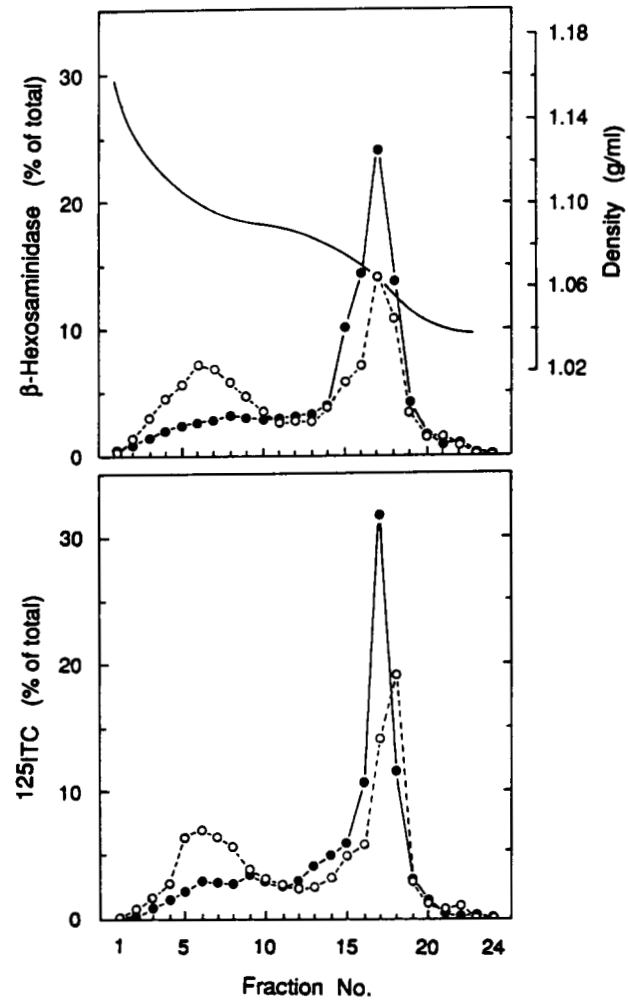

FIG. 6. **Effect of sample layering and dispersion on the distribution of β-hexosaminidase and ^{125}ITC in M + L particles from α-toxin-permeabilized hepatocytes separated in colloidal silica gradients.** Cells were isolated, permeabilized with 32.5 units/ml α-toxin, and incubated for 60 min with ^{125}ITC and an ATP regenerating system. M + L samples were applied to the gradient material by layering (●) or dispersion (○) before centrifugation in an SV-80 rotor as described under "Experimental Procedures."

the midgradient band which prevents autophagic vacuoles in layered samples from attaining their true gradient density (22). On the other hand, when the samples are previously dispersed in the gradient material, density equilibration of the vacuoles occurs before the midgradient band is fully formed (22). For reasons that are not understood, the addition of povidone to colloidal silica is required for the effect; colloidal silica or Percoll alone are apparently not effective (22).

Fig. 5 shows the density distribution of several markers in a hybrid M + L fraction separated on colloidal silica after layering and dispersion. The mixture comprised an 8:1 volume ratio of unlabeled M + L from intact liver and M + L from permeabilized hepatocytes incubated with ^{125}ITC for 30 min. The experiment was designed to compare the distribution of ^{125}ITC from permeabilized cells directly with known distributions of β-hexosaminidase and other markers from intact liver. Two major points are illustrated. First, the densities of β-hexosaminidase, citrate synthase, and galactosyltransferase and their shifts with layering and dispersion (or lack thereof) agree with previous findings in the intact liver (22). These and previous results with more extensive markers (22) indicate that, with dispersion, the shift of autophagic vacuoles is selective and unassociated with the movement of other organelles.

Second, the distributions of ^{125}ITC and β-hexosaminidase in layered and dispersed gradients generally parallel each other. The same was observed in Fig. 6 with permeabilized cells alone, and, in all cases, the amounts shifted to the dense fractions corresponded to losses in the midgradient peak. One difference in Fig. 5 between the intact liver and permeabilized cells may be seen. The peak of ^{125}ITC, which reflects M + L from permeabilized cells, is appreciably lower in density than that of the lysosomal marker. The same lower density is evident for both ^{125}ITC and β-hexosaminidase in gradients from permeabilized cells alone (Fig. 6). The possibility that free ^{125}ITC in the labeled M + L fraction was acquired nonspecifically by M + L particles was excluded in control experiments by the failure of added ^{125}ITC to be taken up by the particles. Although the reason for the density difference in Fig. 5 is not clear, it does suggest that lysosomes from different sources do not interact and can move independently in the gradient.

The correspondence between the dispersion shift of ^{125}ITC and β-hexosaminidase in Fig. 6 indicates that fusion had occurred between AVi and dense bodies. Because AVi would contain ^{125}ITC but not β-hexosaminidase, the enzyme shift would only be seen after fusion had occurred and AVi had matured to

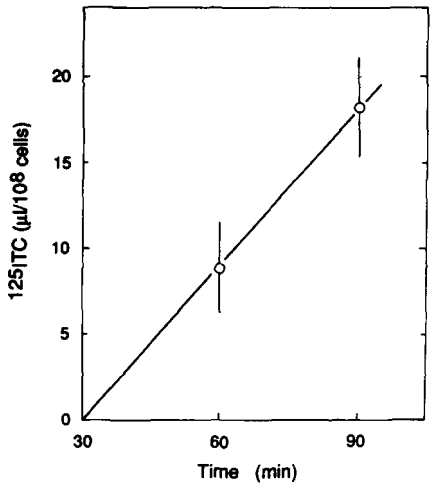

FIG. 7. **Time course of ^{125}ITC uptake into autophagic vacuoles in α-toxin-permeabilized liver cells.** The cells were isolated, permeabilized with 32.5 units/ml α-toxin, and incubated for 90 min with an ATP regenerating system. ^{125}ITC was added at 30 min, and cell samples were taken at 60 and 90 min for the separation of autophagic vacuoles in colloidal silica gradients by the layering-dispersion protocol described in Figs. 5 and 6 and Table III. The results are means ± S.E. of three experiments.

AVd (3, 4). We excluded the possibility that ^{125}ITC in the dense fractions was associated solely with particles that are not osmotically sensitive; in separate experiments (not shown), we found that >50% of the label moved to the top of the gradient when the fractions were diluted 1:1 with water.

Effects of ATP and Nonhydrolyzable GTP Analogs on the Autophagic Uptake of ^{125}ITC in Permeabilized Hepatocytes—Since rates of proteolysis in α-toxin-permeabilized cells appeared to require 15–30 min to stabilize (Fig. 2), ^{125}ITC uptake by autophagic vacuoles, determined by the dispersion shift (Figs. 5 and 6), was measured between 30 and 60 min of cell incubation. As shown in Fig. 7, the time course of ^{125}ITC uptake in control experiments was remarkably linear from 30 to 90 min. Uptake was also found to be directly proportional to ^{125}ITC concentration over a 10-fold range (data not shown).

Energy is clearly required for optimal ^{125}ITC uptake since it was enhanced 75% with the addition of an ATP regenerating system (Table III).

This finding directly confirms an earlier study showing that AVi formation in the hepatocyte is ATP-dependent (32). Although the ATP-dependent ubiquitin pathway is required in stress-induced autophagy, the critical step or steps appear to involve vacuole maturation rather than their formation (33); little is presently known of the initial reactions that utilize ATP. Of importance to our primary objective, though, were the effects of the nonhydrolyzable GTP analogs GTPγS and GMP-PNP (Table III). At doses that were maximally effective in inhibiting proteolysis (see Table IV and Fig. 8 below), they decreased ^{125}ITC uptake between 54 and 60% (Table III). The response to GTPγS appears to require ATP since none was obtained when external ATP was omitted (Table III). 3-Methyladenine was not tested because of its lysosomal density-altering capability, a property related to the fact that it is a weak base (34). This, however, has no bearing on its ability to inhibit AVi formation and has little direct effect on lysosomal proteolysis (24, 34).

Contribution of Endocytosis to the Uptake of ^{125}ITC by Autophagic Vacuoles—In addition to its sequestration by AVi, some ^{125}ITC recovered in autophagic vacuoles (column A, Table III) could have been delivered by (i) fusion of AVi with secondary lysosomes that had acquired the marker through volume/fluid-phase endocytosis or (ii) fusion of AVi directly with fluid-phase endosomes (35, 36). Our results showing that ^{125}ITC uptake is directly proportional to its concentration in the medium appears to exclude receptor-mediated uptake. To evaluate the contribution by endocytosis, we carried out parallel dispersion shift experiments using [*carboxyl*-^{14}C]dextran-carboxyl as a probe; its molecular weight (M_r = 50,000–70,000) would prevent its direct entry into permeabilized cells. The results in column B of Table III show that dextran-carboxyl uptake represented only about 6% of ^{125}ITC uptake under all conditions, a value less than half of the volume fraction of lysosomes that fuse with AVi (37). The fact that the percentage uptake remained unchanged when the macroautophagic component of total autophagy was suppressed by GTPγS suggests that the first pathway (i) is the dominant endocytic route in macro- as well as microautophagy (see Ref. 39 and below). The remainder in column A – B was taken as an index of volume sequestration.

Although absolute quantities of label in the colloidal silica gradients were small, the relative distribution of dextran-car-

TABLE III

Effects of ATP and nonhydrolyzable GTP analogs on the volume uptake of ^{125}ITC and [carboxyl-^{14}C]dextran-carboxyl (DC) into autophagic vacuoles in α-toxin-permeabilized liver cells

Isolated cells were permeabilized by α-toxin (32.5 units/ml) and incubated (10^7 cells/ml) for 60 min under the conditions stated; at 30 min, ^{125}ITC or ^{14}C-labeled DC was added. M + L samples were applied to gradient tubes by layering or dispersion. The increase in radioactivity with dispersion above the corresponding layered value in fractions below the buoyant peak (usually 1–11) was corrected for 0.70 recovery (see "Experimental Procedures") and divided by the initial radioactivity per µl of medium + cells as an index of volume/fluid-phase uptake of ^{125}ITC or of labeled DC by autophagic vacuoles (see Figs. 5 and 6). Except where indicated, the results in columns A and B represent means ± S.E. of 3–9 experiments; ATP-RS, ATP regenerating system.

Additions	ATP-RS	Volume uptake into autophagic vacuoles		
		^{125}ITC (A)	[^{14}C]DC (B)	A – B
		µl h^{-1}/10^8 cells		
None	+	12.99 ± 0.966	0.809 ± 0.115	12.18
None	–	7.44 ± 0.744[a]	0.448 ± 0.072[b]	6.99
GTPγS (1 mM)	–	7.08[c]		
GTPγS (1 mM)	+	5.94 ± 0.187[a]	0.359 ± 0.028[d]	5.58
GMP-PNP (1 mM)	+	5.20[c]	0.380[c]	4.82

[a] $p < 0.001$ *versus* control.
[b] $p < 0.05$ *versus* control.
[c] Single observation.
[d] $p < 0.01$ *versus* control.

TABLE IV

Effects of ATP, GTP, and nonhydrolyzable GTP analogs on proteolysis in α-toxin-permeabilized hepatocytes

Isolated hepatocytes were permeabilized by α-toxin (32.5 units/ml) and incubated for 60 min in cytosolic buffer with 20 µM cycloheximide ± ATP-RS at a density of 2 × 10^6 cells/ml; rates of total valine release were computed between 30 and 60 min; long-lived (autophagic) proteolytic rates were calculated by subtracting from the total an estimate of the extra valine released by nonregulated proteolysis (0.39 µmol of Val $h^{-1}/10^8$ cells; see Table V). The values are means ± S.E. of 3–15 experiments. ATP-RS signifies ATP regenerating system.

Additions	ATP-RS	Proteolysis		
		Total	Long-lived	
		µmol Val $h^{-1}/10^8$ cells		%
None	+	2.39 ± 0.186	2.00	100
None	–	1.36 ± 0.114[a]	0.97	49
GTPγS (1 mM)	+	1.31 ± 0.036[a]	0.92	46
GMP-PNP (500 µM)	+	1.63 ± 0.336	1.24	62
GMP-PNP (1 mM)	+	1.43 ± 0.090[a]	1.04	52
GDPβS (750 µM)	+	1.67 ± 0.048	1.28	64
GDPβS (2 mM)	+	1.39 ± 0.186[b]	1.00	50
GTP (2 mM)	+	2.54 ± 0.222	2.15	108

[a] $p < 0.001$ *versus* control.
[b] $p < 0.005$ *versus* control.

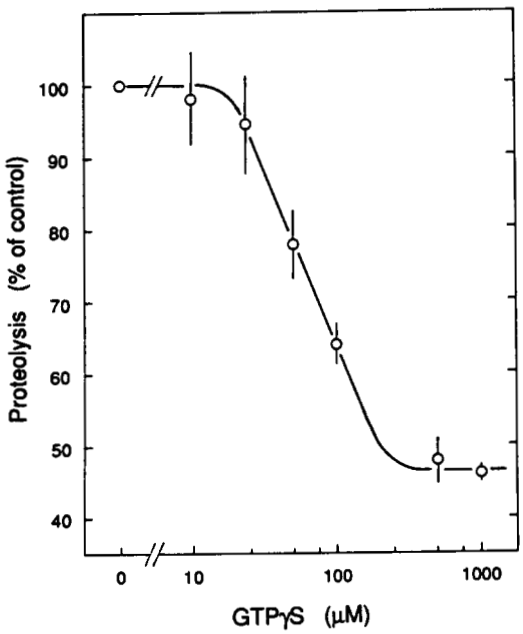

FIG. 8. **Proteolytic responsiveness of α-toxin-permeabilized hepatocytes to GTPγS.** The experiments were carried out as described in Table IV, and the results are means ± S.E. of three to six experiments. Half-maximal inhibition was achieved at 70 μM.

boxyl followed the general pattern seen with ^{125}ITC (not shown). Less, however, was found in the dense fractions and more in the midgradient band. The nature of the vesicles in the midgradient band that contained label after dispersion is not known although endosomes and Golgi vesicles are possibilities; much of the lysosomal marker in this band is believed to be associated with the endoplasmic reticulum (22). The mean rate of total fluid-phase uptake into the M + L fraction of permeabilized cells was 2.27 μl $h^{-1}/10^8$ cells, 67% less than the corresponding value in the intact hepatocyte (38).

Effects of Nonhydrolyzable GTP Analogs on Proteolysis in Permeabilized Hepatocytes; Quantitative Relationship with the Vacuolar Uptake of ^{125}ITC—Results in the first column of Table IV show that maximal inhibitory effects of the nonhydrolyzable GTP analogs GTPγS, GMP-PNP, and GDPβS on total proteolysis were reasonably comparable. In the case of GMP-PNP and GTPγS, 1 mM concentrations were required (Fig. 8), although twice this amount was needed for GDPβS; GTP was without effect. As would be expected from results in Fig. 2, proteolysis was ATP-dependent. It should be emphasized, however, that total valine release in Table IV is not an appropriate measurement for correlating protein degradation with the gradient shift of ^{125}ITC uptake as additional valine is generated from nonregulated sources such as short-lived turnover and endocytosis (1, 3).

As described in the legend of Table V, this problem was circumvented by comparing the *effects* of GTPγS on proteolysis and ^{125}ITC uptake. Because the foregoing sources of valine would be subtracted out, the effects, expressed in fractional terms, should directly reflect autophagic sequestration and the amount of protein degraded. Indeed, the two rates were about equal (1.02–1.03% h^{-1}). Inasmuch as intralysosomal proteolysis is the source of most long-lived valine release in the hepatocyte (1, 6), the autophagic protein/volume ratio, described in the legend to Table V, was used as a factor of proportionality to compute rates of long-lived proteolysis in the presence and absence of GTPγS. In a compilation of earlier data, including the present experiments (reviewed in Ref. 39), the ratio, which expresses the concentration of protein in degradative vacuoles,

TABLE V

Comparative effects of GTPγS on volume sequestration and autophagic protein degradation in autophagic vacuoles of permeabilized liver cells

Rates of autophagic volume uptake (corrected for endocytosis) and total proteolysis were taken from Tables III and IV. The *effects* of GTPγS were directly compared since any release of valine from extraneous sources would be eliminated by difference (3). The mean cytoplasmic volume in 8 control livers was 647 ± 14 μl/10^8 cells, computed as in Ref. 40 and taking 10^8/g as the cell number in livers of *fed* rats (19); hepatocyte protein was 179 ± 3.3 mg and its valine content (105.8 μmol/10^8 cells as determined previously (3). Long-lived (autophagic) proteolysis was calculated from the uptake volumes multiplied by the autophagic protein/volume ratio of the GTPγS effect, 1.086/6.604 or 164.4 nmol/μl (see text). The nonregulated fraction (total *minus* long-lived proteolysis) was 0.39 μmol of Val $h^{-1}/10^8$ cells, with and without GTPγS, in agreement with a similar fraction in the intact cell.[2]

	Control (A)	GTPγS (B)	GTPγS effect	
			A – B	% inhibition
^{125}ITC uptake				
μl $h^{-1}/10^8$ cells	12.181	5.577	6.604	54
% total cytoplasm h^{-1}	1.883	0.862	1.021	
Total proteolysis				
μmol Val $h^{-1}/10^8$ cells	2.394	1.308	1.086	45
% total protein h^{-1}	2.263	1.236	1.026	
Long-lived proteolysis				
μmol Val $h^{-1}/10^8$ cells	2.003	0.917	1.086	54
% total protein h^{-1}	1.893	0.867	1.026	

agreed very closely with the apparent concentration of cytoplasmic protein over the full range of macro- and microautophagy irrespective of whether the sequestration was determined stereologically or from the uptake of ^{125}ITC. In the present study, for example, the protein/volume ratio was 164.4 nmol of Val/μl (Table V) while the apparent cytoplasmic protein concentration was 163.5 nmol of Val/μl, as computed from values in the legend of Table V.

Two important implications can be drawn from the foregoing results. First, the colloidal silica gradient combined with the use of ^{125}ITC appears to provide a valid means for quantitating autophagic sequestration. The principal advantage of the gradient procedure is that autophagic vacuoles can be effectively isolated by the dispersion shift, thus minimizing error from label in other organelles (22). In addition, the use of permeabilized cells makes it possible to measure the accumulation of label in newly formed vacuoles at steady state levels of marker. Seglen and co-workers (41) have reported a parallel between sugar and protein uptake by autophagic vacuoles in electroinjected cells. However, their fractional rates of sugar uptake were significantly higher than those of protein turnover (41, 42), a discrepancy they attributed to an underestimation of cytoplasmic label as a result of its leakage through the plasma membrane (41).

Second, the close agreement between the effects of GTPγS on fractional rates of ^{125}ITC uptake and long-lived proteolysis in Table V suggests that the gradient dispersion maneuver effectively shifts most, if not all, of the macro- and microautophagic vacuoles in the M + L samples into the dense region of the gradient. By itself, though, the agreement would not tell us whether the GTPγS effect was solely limited to macroautophagy or whether microautophagy was involved as well. In approaching this question, the stereologic findings of Table II are of distinct value as shown by the following calculations: the inhibitory effect of GTPγS on the aggregate volume of AVi in Table II was found to be 1.514 μl/10^8 cells. Since AVi are typically 20% larger than AVd, owing mainly to the fall in pH when AVi mature to AVd (3), a closer estimate of the volume of the degradative compartment is 1.514/1.2 or 1.2617. If one assumes that rate constant of vacuole turnover is unaffected by α-toxin treatment, the predicted decrease of the autophagic flux would

be 1.2617 μl/10^8 cells × 0.088 min^{-1} × 60 min = 6.66 μl $h^{-1}/10^8$ cells. This value is nearly identical with the observed effect in Table V and attributable entirely to macroautophagy.

The foregoing assumption is probably correct since the proteolytic effect in Table V (1.086 μmol of Val $h^{-1}/10^8$ cells) divided by the protein pool of the degradative compartment (1.2617 μl/10^8 cells × 163.5 nmol of Val/μl of cytoplasm = 0.2063 μmol of Val) is 5.26 h^{-1} (0.088 min^{-1}), a value equivalent to the corresponding rate constant in the intact parenchymal cell (39).

The failure of GTPγS to inhibit ^{125}ITC uptake and long-lived proteolysis by more than 54% (Table V), while strongly suppressing macroautophagy (Fig. 3), suggests that the dispersion shift contains at least two classes of autophagic vacuoles. In addition to the overt macroautophagic vacuole (1, 3, 4), smaller vacuoles termed type A lysosomes or microautophagic vacuoles have been shown to account for most of the long-lived *basal* protein turnover in liver (40). Although these vacuoles are not regulated by amino acids and are formed by a different membrane mechanism, they share many features with macroautophagic vacuoles, including volume sequestration and the same turnover constant (1, 3, 39, 40). In these experiments, it is probable that virtually all macroautophagic vacuoles and most of the microautophagic variety were retained by the midgradient band in layered gradients, shifting to the dense region with dispersion.

Role of GTP-binding Proteins in Autophagy—The effects of GTPγS on ^{125}ITC uptake and long-lived protein degradation in Table V are fully in accord with the suppression of macroautophagy that was observed by electron microscopy. Although we cannot rule out effects of GTPγS on vacuole fusion or maturation, it is clear from the absence of AVi and AVd in electron micrographs that AVi formation was the primary site of inhibition. Of additional interest is the fact that the relative effectiveness of GTPγS was similar to that observed with maximal amino acid inhibition in isolated cells[2] and in perfused livers from the same animals. This suggests that the proportion of macro- to microautophagy, roughly 54:46, remains relatively constant despite the general decrease in autophagy after permeabilization (Table I). While the dose of GTPγS required for maximal suppression is large compared with the amounts required in isolated vesicles (43), the dose-response agrees with that reported for glucose transporter regulation in α-toxin-permeabilized adipocytes (13).

Our results, which indicate that one or more GTP-binding proteins is required in vacuole formation, could be of value in identifying early events in their formation based on analogous information in other systems. Recent *in vitro* studies, for example, have shown that a small GTP-binding protein Sar1p regulates the initiation of vesicle budding from the ER (10), and, in other studies, a trimeric GTP-binding protein has been implicated in the formation of secretory vesicles from the *trans*-Golgi network (11). Although one, or more, GTP-binding proteins are undoubtedly involved here, their nature is not known. The obvious next step would be to approach these questions in cells permeabilized to proteins. But whether autophagy can be induced after more extensive permeabilization remains to be established.

Acknowledgments—We thank Dr. Sidney Harshman, Dept. of Microbiology, Vanderbilt University School of Medicine, for the generous gift of α-toxin, Dr. Alphonse Leure-duPree and Roland Myers of the Dept. of Neuroscience and Anatomy at Hershey for help with the electron microscopy, and John Wert for excellent technical assistance.

[2] To a first approximation, the nonregulated proteolytic fraction of the intact hepatocyte was determined as follows (see Table V). The maximal inhibitory effect of 10 times (10×) plasma amino acids (46.8 ± 5.6 nmol of Val $min^{-1}/10^8$ cells in five paired experiments, measured as in Table I) was nearly the same as that in perfused livers from similar rats, 46.1 nmol of Val min^{-1}/g (18). The former was divided by the percentage inhibition (57%) in the perfused liver (18) where isotopically measured proteolysis reflects long-lived protein degradation (3). The estimate of long-lived proteolysis was 7.5 nmol min^{-1} less than total valine release (89.6 ± 2.1 nmol $min^{-1}/10^8$ cells, n = 27), a value comparable to the nonregulated fraction of 6.5 nmol of Val min^{-1} or 0.39 μmol h^{-1} (Table V). While more certain measurements of long-lived and nonregulated proteolysis might have been obtained if direct comparisons had been made with previously labeled cells, this was not feasible because of the low cell densities used (see legend to Table I).

REFERENCES

1. Mortimore, G. E., Pösö, A. R., and Lardeux, B. R. (1989) *Diabetes/Metabol. Rev.* **5,** 49–70
2. Hirsimäki, P., Arstila, A. U., Trump, B. F., and Marzella, L. (1983) in *Pathobiology of Cell Membranes* (Arstila, A. U., and Trump, B. F., eds) Vol. 3, pp. 201–235, Academic Press, Orlando, FL
3. Schworer, C. M., Shiffer, K. A., and Mortimore, G. E. (1981) *J. Biol. Chem.* **256,** 7652–7658
4. Dunn, W. A. (1990) *J. Cell Biol.* **110,** 1923–1933
5. Hendil, K. B. (1980) *J. Cell. Physiol.* **105,** 449–460
6. Seglen, P. O. (1987) in *Lysosomes: Their Role in Protein Breakdown* (Glaumann, H., and Ballard, J. F., eds) pp. 371–414, Academic Press, London
7. Hall, A. (1990) *Science* **249,** 635–640
8. Balch, W. E. (1990) *Trends Biochem. Sci.* **15,** 473–477
9. Gomperts, B. D. (1990) *Annu. Rev. Physiol.* **52,** 591–606
10. d'Enfert, C., Wuestehube, L. J., Lila, T., and Schekman, R. (1991) *J. Cell Biol.* **114,** 663–670
11. Barr, F. A., Leyte, A., Mollner, S., Pfeuffer, T., Tooze, S. A., and Huttner, W. B. (1991) *FEBS Lett.* **294,** 239–243
12. Colombo, M. I., Mayorga, L. S., Casey, P. J., and Stahl, P. D. (1992) *Science* **255,** 1695–1697
13. Baldini, G., Hohman, R., Charron, M. J., and Lodish, H. F. (1991) *J. Biol. Chem.* **266,** 4037–4040
14. Bhakdi, S., and Tranum-Jensen, J. (1987) *Rev. Physiol. Biochem. Pharmacol.* **107,** 147–223
15. Harshman, S., Sugg, N., and Cassidy, P. (1988) *Methods Enzymol.* **165,** 3–7
16. Pittman, R. C., and Taylor, C. A., Jr. (1986) *Methods Enzymol.* **129,** 612–628
17. Arion, W. J., Lange, A. J., and Walls, H. E. (1980) *J. Biol. Chem.* **255,** 10387–10395
18. Mortimore, G. E., Khurana, K. K., and Miotto, G. (1991) *J. Biol. Chem.* **266,** 1021–1028
19. Seglen, P. O. (1976) *Methods Cell Biol.* **13,** 29–83
20. Venerando, R., Miotto, G., Kadowaki, M., Siliprandi, N., and Mortimore, G. E. (1991) *FASEB J.* **5,** A1178
21. Burgess, G. M., McKinney, J. S., Fabiato, A., Leslie, B. A., and Putney, J. W., Jr. (1983) *J. Biol. Chem.* **258,** 15336–15345
22. Surmacz, C. A., Wert, J. J., Jr., and Mortimore, G. E. (1983) *Am. J. Physiol.* **245,** C52-C60
23. McEwen, B. F., and Arion, W. J. (1985) *J. Cell Biol.* **100,** 1922–1929
24. Seglen, P. O., and Gordon, P. B. (1984) *J. Cell Biol.* **99,** 435–444
25. Hohman, R. J. (1988) *Proc. Natl. Acad. Sci. U. S. A.* **85,** 1624–1628
26. Kadowaki, M., Pösö, A. R., and Mortimore, G. E. (1992) *J. Biol. Chem.* **267,** 22060–22065
27. Miotto, G., Venerando, R., Khurana, K. K., Siliprandi, N., and Mortimore, G. E. (1992) *J. Biol. Chem.* **267,** 22066–22072
28. Thelestam, M. (1983) *Biochim. Biophys. Acta* **762,** 481–488
29. Kindberg, G. M., Refsnes, M., Christoffersen, T., Norum, K. R., and Berg, T. (1987) *J. Biol. Chem.* **262,** 7066–7071
30. Surmacz, C. A., Ward, W. F., and Mortimore, G. E. (1982) *Biochem. Biophys. Res. Commun.* **107,** 1425–1432
31. Surmacz, C. A., Wert, J. J., Jr., and Mortimore, G. E. (1983) *Am. J. Physiol.* **245,** C61-C67
32. Plomp, P. J. A. M., Gordon, P. B., Meijer, A. J., Høyvik, H., and Seglen, P. O. (1989) *J. Biol. Chem.* **264,** 6699–6704
33. Schwartz, A. L., Brandt, R. A., Geuze, H., and Ciechanover, A. (1992) *Am. J. Physiol.* **262,** C1031-C1038
34. Caro, L. H. P., Plomp, P. J. A. M., Wolvetang, E. J., Kerkhof, C., and Meijer, A. J. (1988) *Eur. J. Biochem.* **175,** 325–329
35. Gordon, P. B., and Seglen, P. O. (1988) *Biochem. Biophys. Res. Commun.* **151,** 40–47
36. Tooze, J., Hollinshead, M., Ludwig, T., Howell, K., Hoflack, B., and Kern, H. (1990) *J. Cell Biol.* **111,** 329–345
37. Surmacz, C. A., Pösö, A. R., and Mortimore, G. E. (1987) *Biochem. J.* **242,** 453–458
38. Ose, L., Ose, T., Reinersten, R., and Berg, T. (1980) *Exp. Cell Res.* **126,** 109–119
39. Mortimore, G. E., and Kadowaki, M. (1994) in *Cellular Proteolytic Systems* (Ciechanover, A. J., and Schwartz, A. L., eds), Wiley-Liss, New York, in press
40. Mortimore, G. E., Lardeux, B. R., and Adams, C. E. (1988) *J. Biol. Chem.* **263,** 2506–2512
41. Kopitz, J., Kisen, G. O., Gordon, P. B., Bohley, P., and Seglen, P. O. (1990) *J. Cell Biol.* **111,** 941–953
42. Seglen, P. O., Gordon, P. B., Tolleshaug, H., and Høyvik, H. (1986) *Exp. Cell Res.* **162,** 273–277
43. Melançon, P., Glick, B. S., Malhotra, V., Weidman, P. J., Serafini, T., Gleason, M. L., Orci, L., and Rothman, J. E. (1987) *Cell* **51,** 1053–1062